+ GEOGRAPHICA
HELVETICA +

supported by
sc | nat

Evolution of fluvial environments and history of human settlements on the Ticino river alluvial plain

Dorota Czerski, Daphné Giacomazzi, and Cristian Scapozza

Institute of Earth Sciences, University of Applied Sciences and Arts of Southern Switzerland (SUPSI),
Campus Mendrisio, Mendrisio, 6850, Switzerland

Correspondence: Dorota Czerski (dorota.czerski@supsi.ch)

Abstract. The present contribution aims to provide better knowledge on the evolution of the fluvial environments of the Ticino river alluvial plain, highlighting the complex interaction of the Ticino river and its lateral tributaries with the human communities since the Neolithic. The study considers information derived from historical sources, from previous research on three sites based in the Ticino river floodplain and from data of six archaeological sites located on four alluvial fans. For the investigated sites the analyses of the lithostratigraphy and the archaeological evidence were constrained with radiocarbon dating, providing the interpretation of the depositional context of the studied sequences and their correlation with the cultural periods and epochs defined for the southern Swiss Alps. The combined approach allowed for the definition of 13 phases of enhanced hydro-sedimentary activity from the Neolithic to the contemporary period. The possible palaeoenvironmental and palaeoclimatic causes, as well as the impacts of these phases on the human settlements, are discussed.

1 Introduction

The rather capricious nature of the upper part of the Ticino river (Switzerland) has been known since ancient times (e.g. Martinoli, 1896; Grossi, 1986). The river originates at the Nufenen Pass at almost 2500 m a.s.l. in the heart of the Alps and flows into Lake Maggiore (193 m a.s.l.) in an almost Mediterranean climate (Scapozza, 2016; Scapozza and Ambrosi, 2021, and references therein). For thousands of years, together with its main tributaries and the streams coming from lateral valleys, the river set the rhythm for the life of the inhabitants of the alluvial plain from Biasca to Magadino (Fig. 1). The major floods have been repeated for centuries and have favoured the lateral displacement of the bed on both sides of the valley, creating new fluvial landforms and also modifying the topography of the floodplain (Scapozza, 2013; Scapozza and Oppizzi, 2013). This capricious behaviour of the Ticino river became increasingly in conflict with human activities until the flood of 1868, which is known as "la grande alluvione" (lit.: the great flood). After this event, it was decided to definitively correct the river and embank it along its entire length (e.g. Martinoli, 1896;

Grossi, 1986; Minor et al., 2004; Piffaretti and Luchessa, 2011; Scapozza, 2013).

The Ticino river dynamics are well known only after the middle of the 19th century (Minor et al., 2004; Piffaretti and Luchessa, 2011). However, information concerning the river dynamics and morphology before its embankment are limited to recent studies, focusing on the sedimentary and geomorphological analysis of the Ticino river floodplain filling (Scapozza and Oppizzi, 2013; Scapozza et al., 2017) or on the analysis of historical documents, with a particular focus on historical cartography, since the Roman Period (Scapozza, 2013). The colonisation history of the bottom of the valley is nevertheless well known thanks to the numerous archaeological discoveries that made possible the reconstruction of the human settlements occupying the Ticino valley since the Neolithic (e.g. Donati, 1986; Crivelli, 1990; De Marinis and Biaggio Simona, 2000; Carlevaro, 2013). In addition to archaeological investigation, the dynamics of the vegetation evolution during the Holocene (with a focus on forest fires) are furthermore well known mostly thanks to palynological studies carried out in ponds, marshes and peat bogs (e.g. Tinner et
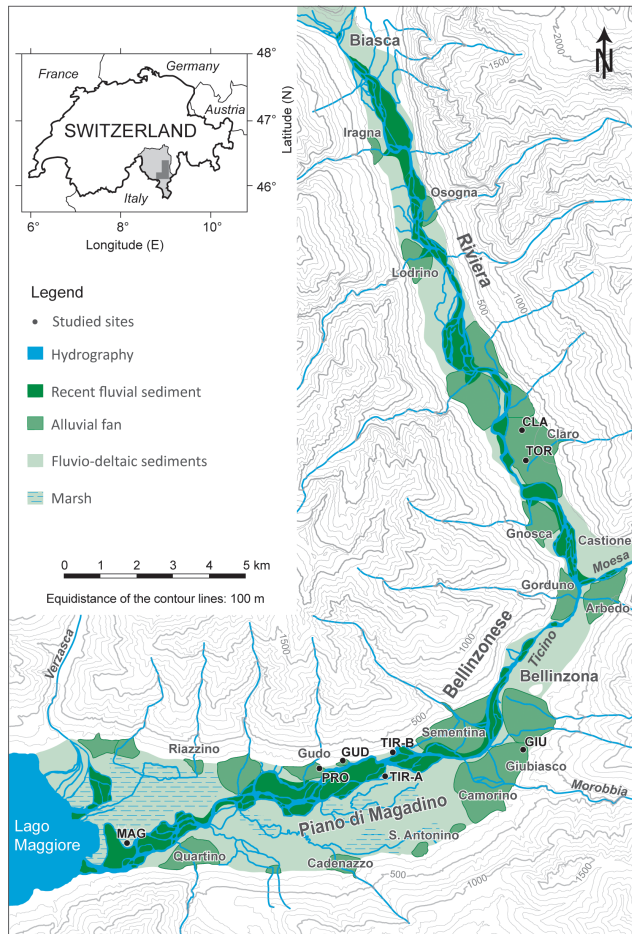
Figure 1. Main hydrographical and geomorphological landforms of the Ticino river floodplain and location of the sites of investigation. Situation of the floodplain in 1854 CE, just before the river embankment of the second half of the 19th century (modified from Scapozza and Oppizzi, 2013). Study sites (from west to east): MAG = Magadino, PRO = Gudo, Progero; GUD = Gudo, Paese, Via alla Chiesa; TIR-A = Gaggiolo Lungo, Gudo; TIR-B = Boschetti, Sementina; GIU = Giubiasco, Palasio; TOR = Claro, Torrazza; CLA = Claro, Longo and In Rasaréi.

al., 1999, 2003; Conedera and Tinner, 2000; Morales-Molino et al., 2015).

In the current context of a climate change which is getting warmer and warmer (Académies suisses des sciences, 2016), it is important to understand the intrinsic relationships between the climate oscillations and the fluvial activity, in particular when the latter increases and can cause repeated floods (e.g. Arnaud et al., 2005; Wirth et al., 2013). Within this framework, the fluvial activity, as well as its environment, is linked to the human communities in terms of resources and natural risks (e.g. Bravard and Petts, 1996; James and Marcus, 2006). Considering also the renewed interest for revitalisation and renaturation projects of fluvial hydrosystems (UFAM, 2017), this study aims to improve our knowl-

edge of past river dynamics and to understand their recent evolution and possibly predict their future dynamics, as was done for other Alpine rivers (e.g. Bravard et al., 1992; Glaser et al., 2005; Laigre et al., 2012). The main objective is to determine the morphosedimentary dynamics of the Ticino river and its tributaries, as well as their interaction with the human communities, since the Neolithic. It will be achieved through the study of fluvial deposits in archaeological sites thanks to the following evaluations: (1) the definition of phases of enhanced hydro-sedimentary activity; (2) the analysis of their palaeoenvironmental and palaeoclimatic causes; and (3) the determination of their relationships with the human communities in terms of protection from the floods and impact of this natural phenomenon on anthropic constructions.

2   Study area

The Ticino fluvio-deltaic plain includes the Ticino river floodplain between Biasca (confluence of Ticino and Brenno rivers) and Giubiasco (valley bottom of the Riviera and Bellinzonese), as well as the Ticino (and Verzasca) river delta between Camorino and Lake Maggiore, known as Piano di Magadino (Fig. 1). In the upper part (Riviera), the valley is oriented north-northwest–south-southeast. Despite its embankment, the current morphology of the Ticino river through Riviera is meandering between the lateral alluvial fans which force the watercourse to switch from the right side to the left side of the valley, and vice versa. The width of the floodplain rarely exceeds 1 km and contracts to a few hundreds of metres near the distal part of the alluvial fans. Between Gnosca and Gorduno, the valley is oriented north–south. The Ticino river is constrained by the action of the Moesa river (tributary on the left side of the Ticino river) and by the presence of the Arbedo and Gorduno alluvial fans, facing each other and occupying the valley. From Gorduno, the valley forms a bend and is oriented northeast–southwest until Camorino. As upstream, the morphology is conditioned by the presence of impressive alluvial fans. Downstream from the confluence between the Ticino river and the Morobbia river, the floodplain is oriented east–west until Lake Maggiore. The current fluvial morphology is characterised by a single straight channel due to the river embankment.

The Piano di Magadino is a huge fluvio-deltaic plain formed by the progradation of the Ticino and Verzasca deltas during the Holocene (Scapozza and Oppizzi, 2013; Scapozza, 2016; Scapozza and Czerski, 2019; Scapozza and Ambrosi, 2021). Its width is variable from 2.5 km in the narrowest sectors to 3.5 km in the widest sector. The great mobility of the active band of the Ticino river during the Late Holocene, as well as the relatively frequent floods (e.g. Scapozza, 2013; Scapozza and Oppizzi, 2013), has favoured the development of the settlements on the structural terraces on the lower part of the valley sides or on the alluvial fans of the tributaries (e.g. Carlevaro, 2013).

This study considers information coming from three sites described in previous research concerning the sedimentary filling of the Ticino river floodplain (Scapozza and Oppizzi, 2013; Scapozza, 2016; Scapozza et al., 2017), as well as information from six archaeological sites located on four alluvial fans of the Ticino river tributaries, which have been the subject of recent excavations (Cardani Vergani, 2018, 2020, 2021; Scapozza and Czerski, 2019).

The three sites located on the Ticino river floodplain are based in Magadino (noted MAG in this study), in Gaggiolo Lungo (TIR-A) and in Boschetti (TIR-B). The six archaeological sites are described in more detailed below.

The site of Gudo, Santa Maria (locality of Progero, PRO), is located on the alluvial fan fed by the streams coming from the Valle di Progero and just above Gudo (Cardani Vergani, 2018; Scapozza and Czerski, 2019). It presents a Bronze Age settlement.

In Gudo, a second site is studied in Via alla Chiesa (GUD). It is located on the alluvial fan at the bottom of Valle del Cugnolo. Structures of the Iron Age were discovered there, including an imposing L-shaped wall (Cardani Vergani, 2018; Scapozza and Czerski, 2019).

In Giubiasco (GIU), in the historic nucleus of Palasio (gardens of Villa Rusconi), on the alluvial fan of the Fossato-Sbardella stream, traces of occupation since the Bronze Age were discovered particularly with remains of structures and buildings from the Roman Period to the end of the 18th century (Cardani Vergani, 2020, 2021). The Fossato-Sbardella stream (Italian "Riale Fossato-Sbardella", also known as Palasio stream, "ruscello del Palasio" in Italian) was at the origin of floods causing considerable damages during the last centuries (Documentazione IVS Cantone Ticino, 1999).

In the locality of Claro, three archaeological sites were investigated. The two sites of "Longo" (CLA-L) and of "In Rasaréi" (CLA-R) presented structures of the Neolithic and of the Iron Age (Cardani Vergani, 2019, 2020, 2021); the site "Longo", in particular, was the scene of the discovery of a megalithic site unique for the south of the Alps (Cardani Vergani, 2020, 2021). In the site of "Scerese" in the hamlet of Torrazza (TOR), in addition to the discovery of an Early Iron Age settlement, a 20 m long and 3–4 m high trench was opened on the fluvial deposits forming the near-surface part of the alluvial fan of Claro (Cardani Vergani, 2020), which is the largest in the Canton of Ticino and whose development after the last deglaciation has been the subject of recent studies (Scapozza, 2016; Carlevaro et al., 2017; Scapozza and Czerski, 2019).

3 Materials and methods

3.1 Sedimentological description

Sedimentological descriptions are based on lithofacies codes proposed by Miall (1977a, b) for the characterisation of fluvial depositional environments, with the modifications pro-

Colour	Name	CMYK	RGB	Hex
	dark grey	0-0-0-75	100-99-99	#646363
	grey	0-0-0-50	157-157-156	#9D9D9C
	light grey	0-0-0-25	208-208-208	#D0D0D0
	dark brown	40-50-80-60	61-51-20	#3D3314
	brown	40-50-80-30	107-89-36	#6B5924
	light brown	40-50-80-0	153-128-51	#998033
	dark beige	30-40-60-0	179-153-102	#B39966
	beige	15-30-60-0	217-179-102	#D9B366
	light beige	9-12-60-0	232-224-102	#E8E066

Figure 2. Colour codes for the deposit descriptions used in this study (Figs. 4–6). Source: field chart of the Swiss Association of Geologists CH-GEOL.

posed by Schoeneich (1998) and Scapozza et al. (2009) (Table 1). Lithofacies allow a direct description of the texture (G = gravel, S = sand, F = fine sediments), the matrix structure (m = matrix supported, c = clast supported) and the sedimentary structure(s), as well as stratification, lamination, normal or inverse grading, etc. The lithofacies codes make it possible to link the deposits with the sedimentation environment and/or process and therefore to interpret its genesis. The matrix colour of the deposits is based on the field chart of the Swiss Association of Geologists CH-GEOL (Fig. 2). When the colour of the deposit is not specified, it is because the information is missing or because there is no matrix. Grain size description is based on grain size classes defined by Cailleux and Tricart (1963) and modified by King (1966): boulders (> 200 mm), cobbles (200–60 mm), coarse gravel (60–20 mm), medium gravel (20–6 mm), fine gravel (6–2 mm), coarse sand (2–0.6 mm), medium sand (0.6–0.2 mm), fine sand (0.2–0.06 mm), silt (0.06–0.002 mm) and clay (< 0.002 mm).

The sedimentological descriptions are presented in Sect. 4.2 (Figs. 4–6). A defined legend of patterns was used depending on the origin and the grain size of the deposit (Fig. 3). The represented thickness of the deposit layers is relative. Therefore, the scale used for the stratigraphic representations is not a function of a depth scale but depends on a timescale. Three of the stratigraphic representations are based on core logging, while all the others sites have been described from a section or a trench.

3.2 Radiocarbon dating

The age and stratigraphy of the deposits were determined using the radiocarbon dating method on organic matter debris and charcoals. Radiocarbon dating was performed by accelerator mass spectrometry (AMS) technique by the laboratories in Poznań, Poland (Poznań Radiocarbon Laboratory, laboratory codes: Poz-*), and in Miami, Florida (Beta Analytic Inc, laboratory codes: Beta-*). Radiocarbon ages measured and corrected with $\delta^{13}C$ (conventional ages) are expressed in radiocarbon years before present (a ^{14}C BP), whereas the calibrated ages are expressed in calendar years

Table 1. Lithofacies codes for the deposits description used in this study. Modified from Miall (1977a, b), Schoeneich (1998), and Scapozza et al. (2009).

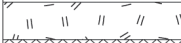| Facies code	Lithofacies	Sedimentary structures	Interpretation
Gmc	Massive, clast-supported cobbles and/or gravel (but with matrix)	Horizontal bedding, imbrication	Braided river deposit in an active band composed by gravelly sandy banks
Gmm	Massive, matrix-supported cobbles and/or gravel	None	Bimodal transport, mass transport (debris flow)
Gt	Cobbles and/or gravel, stratified	Trough crossbeds	Minor channel fills
Sm	Massive sand	None	Channel bottom filling
Sm(c)	Massive sand with sparse coarse clasts	None	Channel bottom filling
Sp	Planar crossbedded sand	Planar crossbeds	Transverse bars, sand waves (lower flow regime)
Sl	Laminated sand	Low-angle ($< 10°$) crossbeds or horizontal lamination	Scour fills
Sh	Sand, very fine to very coarse, may be gravelly	Horizontal lamination, parting or streaming lineation	Planar bed flow in secondary channel or extra-channel
Fm	Massive fine sediment (silt, clay)	None	Rapid decantation overbank or by drape deposit (swamp/pond deposit; colluvium)
Fl	Laminated fine sediment (silt, clay)	Fine horizontal lamination, very small ripples	Overbank or waning flood deposits (rapid decantation)
A	Anthropic structure	None	Structure built from human activity
P	Pedogenetic unit	Primary structure modified by pedogenesis	Soil, palaeosoil
R	Backfilling, arable, man-made sensu lato	None	Human activity
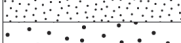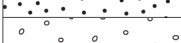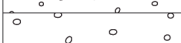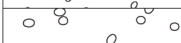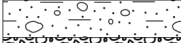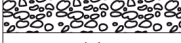
Pattern	Name
	soil (root)
	organic material
	clay
	silt
	fine sand
	medium sand
	coarse sand
	gravel 2–5mm
	gravel 5–10mm
	gravel 10–25mm
	gravel 25–63mm
	moraine
	anthropic structure
	sample

Figure 3. Legend of the patterns used for the stratigraphic logs in this study (Figs. 4–6).

before present (a cal BP) or with the notation CE (common era) or BCE (before the common era). Reference geochronology, cultural chronology, climate oscillations and other regional proxies are also expressed in years (a) or millennia (ka) *before 2000 CE* (noted as "b2k"). Conventional age calibration was performed with OxCal 4.4 software of the Oxford Radiocarbon Accelerator Unit (Bronk Ramsey, 2001, 2020) using the IntCal20 curve (Reimer et al., 2020) and with a 2σ confidence interval (95.4 % of probability).

3.3 Geoarchaeological observations and phase dating

The sedimentological characterisation of the deposits was combined with archaeological observations and dating, allowing for the interpretation of the depositional context of the studied sequences. Relative dating coming from the archaeological seriation of assemblages and artefacts discovered on study sites was confirmed by radiocarbon dating or, in the absence of numerical dating, was used for completing the chronostratigraphy of the described sedimentary sequences (Moscato, 2002). Both numerical dating by radiocarbon and

Table 2. Chronology of cultural periods in the southern Swiss Alps. Source: (1) Tinner et al. (2003:1454); (2) Carlevaro (2013:12).

Cultural period	Age	Epoch	Source
Neolithic	5500–2200 BCE		1
Early Bronze Age	2200–1550 BCE		1
Middle Bronze Age	1550–1300 BCE		1, 2
Late Bronze Age	1300–900 BCE	Canegrate (1300–1200 BCE) Protogolasecca I–II (1200–1000 BCE) Protogolasecca III (1000–900 BCE)	2
Early Iron Age	900–450 BCE	Golasecca IA1 (900–825/800 BCE) Golasecca IA2–IC (825/800–625 BCE) Golasecca IIA/B/TI A (625–550 BCE) Golasecca IIB–IIIA1/TI B/C (550–450 BCE)	2
Late Iron Age	450–15 BCE	Golasecca IIIA2/A3/TI D–La Tène B (450–280/250 BCE) La Tène C–La Tène D1 (280/250–70/80 BCE) La Tène D2–Augustan epoch (70/80–15 BCE)	2
Roman Period	15 BCE–375 CE	Augustan–Tiberian epoch (15 BCE–37 CE)	1, 2
Migration Period	375–568 CE		1
Early Middle Ages	568–1000 CE		
High Middle Ages	1000–1250 CE		
Late Middle Ages	1250–1492 CE		
Modern period	1492–1789 CE		
Contemporary period	1789 CE–today		

archaeological seriation were integrated in a chronology of cultural periods and epochs defined for the southern Swiss Alps (Table 2).

With the exception of radiocarbon dating of wood or charcoal remains from hearths of anthropic settlements, all the other numerical datings were performed on charcoals or organic matter within the deposits matrix. Therefore, the resulting age cannot be considered as an event age but must be interpreted as a bulk age (Strunk et al., 2020). As a consequence, the entire time span of the calibrated age was used to define the events chronostratigraphy. In the following sections, in some cases just the median calibrated age is mentioned in order to simplify the lecture by the reader. In the case of a coarse fluvial deposits embedded in dated fine colluvium deposits and/or in palaeosoils, the age constraint of the period of enhanced stream activity was determined by the younger terminus of the lower unit and by the older terminus of the upper unit. Concerning the periods of construction with human settlement, they are assumed to be periods of low river activity. In the absence of numerical dating of the building elements, the age constraint was determined from the bulk age of the soil on which the structure was built and from the bulk age of the fluvial deposit related to the flood impacting the structure. As a consequence, the defined chronostratigraphy is not based on direct numerical dating

of the phases of enhanced hydro-sedimentary activity or of the construction phases but rather on the definition of a time interval between a terminus post quem ("limit after which") and a terminus ante quem ("limit before which") (Moscato, 2002; Grant et al., 2015).

4 Results

4.1 Radiocarbon dating

The radiocarbon dating analyses presented in this contribution were performed on 27 samples: 21 collected on the archaeological sites PRO, GUD, GIU, CLA and TOR (Fig. 1) and 6 associated with the previous study sites MAG and TIR (Fig. 1; Scapozza and Oppizzi, 2013; Scapozza et al., 2017). Table 3 presents the name, the location and the type of sample, whereas Table 4 shows the analysis results and calibration for radiocarbon dating of each sample.

4.2 Field observations

4.2.1 Bolle di Magadino (MAG)

The stratigraphy presented for the site Bolle di Magadino (Fig. 1, MAG) is based on a borehole of 50 m described in a previous study (Scapozza and Oppizzi, 2013). From bottom

Table 3. Nomenclature, location and characteristics of the 27 samples dated by radiocarbon in this study. The sites are listed from the west to east as they are represented in Fig. 1. Source: (1) Scapozza and Oppizzi (2013); (2) SUPSI Institute of Earth Sciences; (3) Scapozza et al. (2017); (4) Briva Sagl Archeologia e Patrimonio, with the authorisation of the Ufficio dei beni culturali, Repubblica e Cantone del Ticino, Bellinzona.

Sample name	Sample code	Locality, district	Coordinate [CH1903 + /LV95]		Dated material	Source
			X	Y		
MAG_1	Poz-31086	Magadino, Castellaccio	2 710 790	1 112 340	Wood	1
MAG_2	Poz-31083	Magadino, Castellaccio	2 710 790	1 112 340	Wood	1
MAG_3	Poz-31077	Magadino, Castellaccio	2 710 790	1 112 340	Wood	1
PRO_1	Beta-488655	Gudo, Progero	2 716 190	1 114 560	Charcoal	2
GUD_1	Beta-462310	Gudo, Paese	2 716 715	1 114 800	Charcoal	2
GUD_2	Beta-462309	Gudo, Paese	2 716 715	1 114 800	Charcoal	2
GUD_3	Beta-462308	Gudo, Paese	2 716 715	1 114 800	Charcoal	2
GUD_4	Beta-462311	Gudo, Paese	2 716 715	1 114 800	Charcoal	2
GUD_5	Beta-462312	Gudo, Paese	2 716 715	1 114 800	Charcoal	2
TIR_1	Beta-441296	Sementina, Boschetti	2 718 320	1 114 930	Organic silt	3
TIR_2	Beta-443897	Gudo, Gaggiolo lungo	2 718 010	1 114 310	Organic silt	3
TIR_3	Beta-441293	Gudo, Gaggiolo lungo	2 718 010	1 114 310	Wood pole	3
GIU_1	Poz-114639	Giubiasco, Palasio	2 721 940	1 114 933	Charcoal	2
GIU_2	Poz-114629	Giubiasco, Palasio	2 721 924	1 114 935	Hearth's remains	2
GIU_3	Poz-114640	Giubiasco, Palasio	2 721 942	1 114 933	Charcoal	2
GIU_4	Beta-563001	Giubiasco, Palasio	2 721 950	1 114 950	Charcoal	4
GIU_5	Poz-114628	Giubiasco, Palasio	2 721 937	1 114 930	Charcoal	2
TOR_1	Poz-114890	Claro, Torrazza	2 721 980	1 123 440	Charcoal	2
TOR_2	Poz-114630	Claro, Torrazza	2 721 980	1 123 440	Charcoal	2
TOR_3	Poz-114624	Claro, Torrazza	2 721 980	1 123 440	Charcoal	2
TOR_4	Poz-114889	Claro, Torrazza	2 721 980	1 123 440	Charcoal	2
CLA_1	Beta-533230	Claro, Paese	2 721 840	1 124 225	Charcoal	4
CLA_2	Beta-533229	Claro, Paese	2 721 840	1 124 225	Charcoal	4
CLA_3	Beta-562999	Claro, Paese	2 721 875	1 124 120	Charcoal	4
CLA_4	Beta-522007	Claro, Paese	2 721 840	1 124 225	Charcoal	4
CLA_5	Beta-563000	Claro, Paese	2 721 875	1 124 120	Charcoal	4
CLA_6	Beta-533231	Claro, Paese	2 721 840	1 124 225	Charcoal	4

to the top, the simplified log (Fig. 4a) changes from a massive layer of sand with silt (Sm-Fm) to a laminated deposit of silt with fine sand (Fl), indicating a confined environment of deposit. It is followed by a thick sequence of fluvio-deltaic deposits which is dominated by massive sands (Sm), some with massive (Fm) or laminated (Fl) silt, alternated with stratified medium to coarse sands (Sp). An important change in the nature of the deposits is observed in the upper part of the log, with the appearance of a coarser layer with sandy gravel (Gmm) or with silty sand (Sm-Fl) of fluvial origin, suggesting the migration of the main fluvial channel and/or the increase in the solid transport energy.

The radiocarbon dating was performed on wood material found in three different layers. Two of the organic samples were located on both sides of a deposit representing a phase of enhanced hydro-sedimentary activity, while the third one was directly collected inside it (Fig. 4a and Table 3). Therefore, two phases of enhanced hydro-sedimentary activity were defined. The first phase is constrained between

680 CE (lower limit for sample MAG_2) and 960 CE (upper limit for sample MAG_1, Table 4), and the second one corresponds to the range of radiocarbon ages resulting from sample MAG_3, dated between 1690 and 1920 CE. These two phases are respectively attributed to the Early Middle Ages and the modern period.

4.2.2   Gudo, Progero (PRO)

At the site Gudo, Progero (Fig. 1, PRO), two main phases of enhanced hydro-sedimentary activity directly related to coarse alluvial deposits could be observed. The first phase consists of a palaeochannel at the bottom of the stratigraphy, classified as Gmc (Table 1 and Fig. 4b). The fine sandy to silty layers (Sm-Fm) overlaying it indicate a calm period which was dated by radiocarbon geochronology on charcoal (Fig. 4b and Table 3, PRO_1). The following second alluvial phase shows many events with coarse material deposits succeeding and crosscutting each other, described as Gmc,

Table 4. Laboratory results and calibration of the 27 radiocarbon datings analysed in this study. The sites are listed from the west to the east as presented in Fig. 1. For the location and characteristics of the samples, see Table 3.

| Sample name	Sample code	Conventional age [a^{14}C BP]	Calibrated age [a cal BP]	Calibrated age [BCE/CE]	Median calibrated age [BCE/CE]
MAG_1	Poz-31086	1185 ± 30	1250–1230 (0.2 %) 1180–1050 (86.5 %) 1040–990 (8.7 %)	700–720 CE (0.2 %) 770–900 CE (86.5 %) 910–960 CE (8.7 %)	840 CE
MAG_2	Poz-31083	1235 ± 30	1270–1060 (95.4 %)	680–890 CE (95.4 %)	800 CE
MAG_3	Poz-31077	50 ± 30	260–220 (27.3 %) 140–30 (68.1 %)	1690–1730 CE (27.3 %) 1810–1920 CE (68.1 %)	1830 CE
PRO_1	Beta-488655	3110 ± 30	3400–3230 (95.4 %)	1450–1280 BCE (95.4 %)	1380 BCE
GUD_1	Beta-462310	2440 ± 30	2700–2630 (22.3 %) 2620–2560 (10.9 %) 2540–2350 (62.3 %)	760–680 BCE (22.3 %) 670–610 BCE (10.9 %) 600–400 BCE (62.3 %)	540 BCE
GUD_2	Beta-462309	2250 ± 30	2350–2290 (30.5 %) 2270–2150 (64.9 %)	400–340 BCE (30.5 %) 320–200 BCE (64.9 %)	280 BCE
GUD_3	Beta-462308	2180 ± 30	2320–2090 (95.4 %)	370–150 BCE (95.4 %)	270 BCE
GUD_4	Beta-462311	2060 ± 30	2120–1930 (95.4 %)	170 BCE–20 CE (95.4 %)	70 BCE
GUD_5	Beta-462312	1630 ± 30	1570–1400 (95.4 %)	380–550 CE (95.4 %)	430 CE
TIR_1	Beta-441296	1230 ± 30	1270–1200 (27.7 %) 1190–1060 (67.7 %)	680–750 CE (27.7 %) 760–890 CE (67.7 %)	800 CE
TIR_2	Beta-443897	560 ± 30	640–580 (48.6 %) 570–520 (46.9 %)	1310–1370 CE (48.6 %) 1380–1430 CE (46.9 %)	1360 CE
TIR_3	Beta-441293	100 ± 30	270–210 (26.1 %) 150–20 (63.3 %)	1680–1740 CE (26.1 %) 1800–1930 CE (69.3 %)	1840 CE
GIU_1	Poz-114639	825 ± 30	780–680 (95.4 %)	1170–1270 CE (95.4 %)	1230 CE
GIU_2	Poz-114629	705 ± 30	690–630 (76.5 %) 590–560 (18.9 %)	1260–1320 CE (76.5 %) 1360–1390 CE (18.9 %)	1290 CE
GIU_3	Poz-114640	470 ± 30	550–490 (95.4 %)	1400–1460 CE (95.4 %)	1440 CE
GIU_4	Beta-563001	330 ± 30	480–310 (95.4 %)	1470–1640 CE (95.4 %)	1560 CE
GIU_5	Poz-114628	145 ± 30	290–1950 (95.4 %)	1660–1950 CE (95.4 %)	1810 CE
TOR_1	Poz-114890	4680 ± 30	5480–5310 (95.4 %)	3530–3360 BCE (95.4 %)	3440 BCE
TOR_2	Poz-114630	2705 ± 30	2860–2750 (95.4 %)	910–800 BCE (95.4 %)	860 BCE
TOR_3	Poz-114624	2700 ± 30	2860–2750 (95.4 %)	910–800 BCE (95.4 %)	850 BCE
TOR_4	Poz-114889	2005 ± 30	2010–1830 (95.4 %)	60 BCE–120 CE (95.4 %)	10 CE
CLA_1	Beta-533230	4240 ± 30	4870–4800 (62.4 %) 4760–4700 (27.6 %) 4680–4650 (5.5 %)	2920–2850 BCE (62.4 %) 2810–2750 BCE (27.6 %) 2730–2700 BCE (5.5 %)	2880 BCE
CLA_2	Beta-533229	4060 ± 30	4800–4760 (6.3 %) 4690–4680 (0.3 %) 4630–4420 (88.8 %)	2850–2810 BCE (6.3 %) 2740–2730 BCE (0.3 %) 2680–2470 BCE (88.8 %)	2590 BCE
CLA_3	Beta-562999	3990 ± 30	4530–4400 (95.4 %)	2580–2460 BCE (95.4 %)	2520 BCE
CLA_4	Beta-522007	3940 ± 30	4520–4480 (10.2 %) 4450–4280 (82.8 %) 4270–4250 (2.5 %)	2570–2530 BCE (10.2 %) 2500–2340 BCE (82.8 %) 2330–2300 BCE (2.5 %)	2430 BCE
CLA_5	Beta-563000	3270 ± 30	3570–3440 (89.3 %) 3430–3400 (6.2 %)	1620–1490 BCE (89.3 %) 1480–1450 BCE (6.2 %)	1530 BCE
CLA_6	Beta-533231	2600 ± 30	2770–2700 (95.4 %)	820–750 BCE (95.4 %)	790 BCE
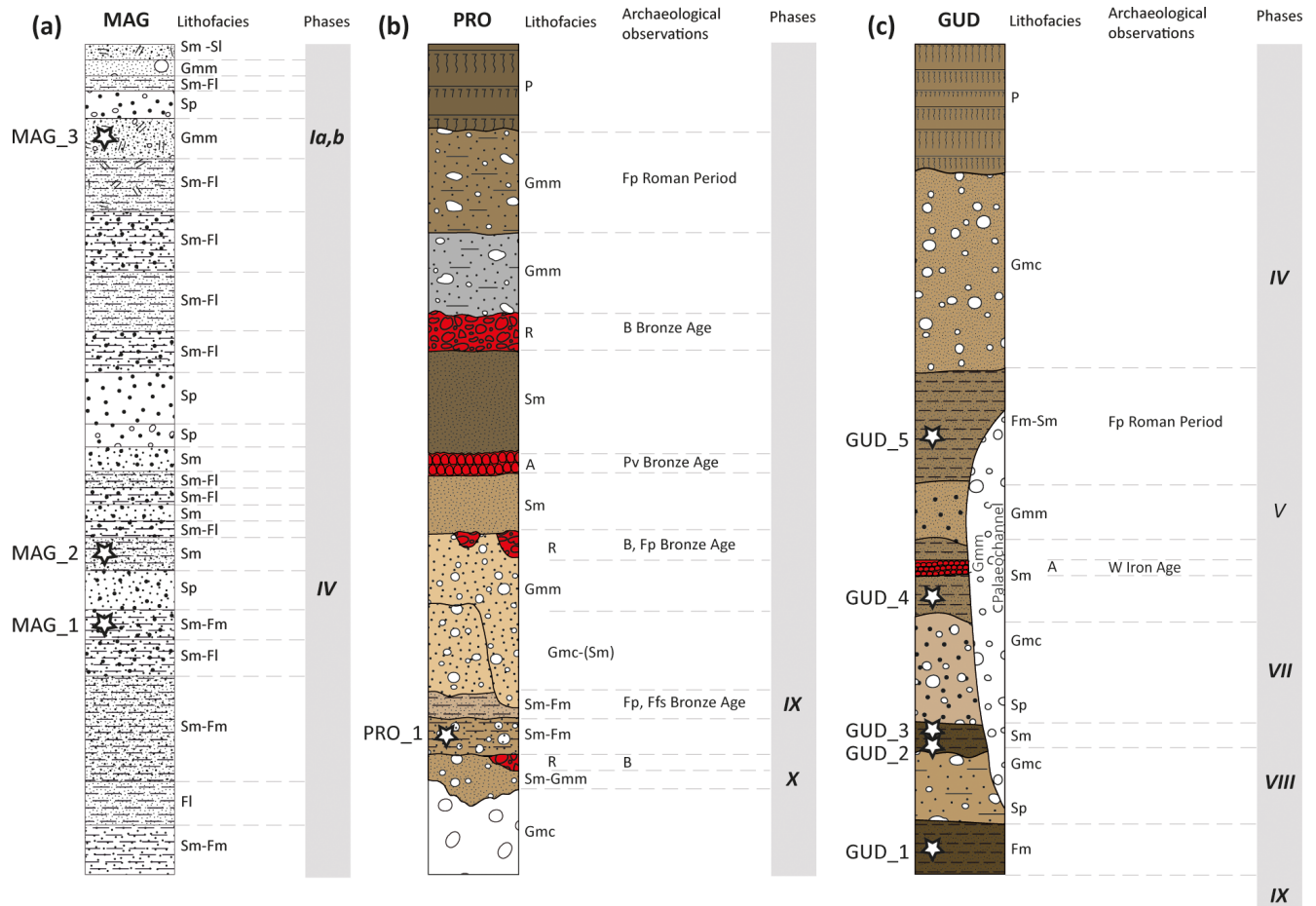
Figure 4. Stratigraphic logs in a timescale representation, with their corresponding lithofacies and archaeological remains. The phases (grey shaded) correspond to the enhanced hydro-sedimentary phases defined in Sect. 5.1. Sites: **(a)** Bolle di Magadino (MAG; Scapozza and Oppizzi, 2013); **(b)** Gudo, Progero (PRO); **(c)** Gudo, Paese (GUD). Codes for archaeological observations: B = backfilling; Ffs = fragments of flint stone; Fp = fragments of pottery; Pv = pavement; W = wall.

Sm and Gmm. These deposits are attributed to the lateral alluvial fans or debris flows from the valley slope. After this phase, the first records of human settlement in the area are observed and consist of anthropic backfillings containing some ceramic debris of the Bronze Age. It is then followed by two events of finer sandy deposits (Sm) which alternate with remnants of human constructions still dating from the Bronze Age. These deposits are of fluvial origin and attributed to a possible temporary palaeomeander of the Ticino river, which allowed the sudden deposition of very fine and homogeneous material by rapid decantation. The presence of anthropic pavements at that time confirms the proximal position of the human settlements to the river (both the stream from the valley slope and the Ticino river), confirmed also by the presence, less than 100 m to the south, of the protohistoric necropolis of Gudo (Sormani, 2007, 2012, 2013).

The radiocarbon age determined for the sample PRO_1 between 1450 and 1280 BCE (Table 4) and attributed to the Late Bronze Age is coherent with the fragments of pottery of

the Bronze Age described in the overlying deposits of anthropic origin (Fig. 4b) (Cardani Vergani, 2018; Scapozza and Czerski, 2019).

The two phases of hydro-sedimentary activity deduced from the stratigraphic sequence of PRO and subsequently constrained by the radiocarbon dating of charcoal within the finer deposits can be chronologically resumed as follows: a phase during the Middle Bronze Age and a phase during the Late Bronze Age and Early Iron Age (Fig. 4b).

4.2.3   Gudo, Paese (GUD)

This site (Fig. 1, GUD) is located in a more proximal position to the slope compared to the site Gudo, Progero (Fig. 1, PRO).

Four layers with coarser grain size deposits were observed, suggesting the record of four events of major hydro-sedimentary activity in the area. The deposits of the first and second events are defined as Sp and Gmc towards the

top of the layer (Table 1 and Fig. 4c), indicating an increase in the energy of the fluvial transport. The overlying coarser deposits are considered as Gmm and Gmc. They are attributed to fluvial active channels of the alluvial fan, with hyperconcentrated deposits coming from the slope of the Ticino valley. The deposits related to the four events of enhanced hydro-sedimentary activity alternate with finer sediments (Fm and Sm) associated with periods of low river activity, which allowed a soil development (pedogenesis). Some charcoals found in those finer layers were sampled for the radiocarbon dating analysis (Fig. 4c and Table 3, GUD_1–GUD_5).

The radiocarbon ages determined for the samples of GUD show time ranges between 760–400 BCE (GUD_1) and 380–550 CE (GUD_5, Table 4), covering a period including the Early Iron Age, the Roman Period and the Migration Period. The four events of enhanced hydro-sedimentary activity observed could have occurred in this interval of time and can be chronologically placed as follows: two phases during the Late Iron Age, a phase during the Roman Period and a phase during the Early Middle Ages (Fig. 4c). The archaeological findings are coherent with the radiocarbon ages; in particular, the L-shaped wall of the Iron Age found between the first two events confirms the dating and suggests a stable human settlement in the area during the Iron Age, as well as the need to build a dam for containing the floods, most likely coming from the Ticino river (Cardani Vergani, 2018; Scapozza and Czerski, 2019).

4.2.4 Ticino river floodplain (TIR)

The data for the Ticino river floodplain (Fig. 1, TIR) derive from previous studies (Scapozza et al., 2017). For the present contribution, two stratigraphic sequences typical for the Ticino river alluvial plain are shown, coming from the locality Gaggiolo Lungo in Gudo (TIR-A) and from the Boschetti area in Sementina (TIR-B).

The stratigraphy of TIR-A was described in an excavation trench of 3 m height (Fig. 5a). Nine units of natural deposits of swamp-fluvial origin were observed: silty layers more or less rich in organic material (Fm) alternated with silty sands (Sm). The peculiarity of the site consists of the finding of a wooden pole (sample TIR_3, Table 3) embedded in a swamp deposit (Fm) at the bottom of the stratigraphy (TIR_2). This wooden pole was subsequently covered by sandy fluvial deposits. The difference between the radiocarbon ages for the two samples, 1680–1930 CE for TIR_3 and 1310–1430 CE for TIR_2 (Table 4), dates the period of calm before the subsequent enhanced hydro-sedimentary activity phase which occurred after 1680 CE, as shown by the interval of ages determined for TIR_3.

The stratigraphy of TIR-B derives from a borehole of 8 m (Fig. 5b). From the bottom to the top, the sequence alternates between finer sediments (Sp, Fm, Sm) and coarser deposits (Gmc, Gmm). This is due to the river dynamics which are going from calmer and confined environments such as extra-channels or swamps to fluvial active channels.

Sample TIR_1 was collected for radiocarbon dating from a fine organic layer (Fm) underlying a coarse deposit (Fig. 5b and Table 3). TIR_1 dated between 680 and 890 CE (Table 4) provides the interval of time during the Early Middle Ages, corresponding to the start of the enhanced hydro-sedimentary activity phase observed in the sequence.

4.2.5 Giubiasco, Palasio (GIU)

In Giubiasco, Palasio (Fig. 1, GIU), the activity and position of the Fossato-Sbardella stream had a determinant influence on the sequence of deposits and the construction and destruction phases observed (Cardani Vergani, 2020, 2021). The observations are resumed in a representative stratigraphic sequence with 10 units of natural deposits and five levels of anthropic structures (Fig. 5c and Table 3).

The stratigraphic sequence starts with a deposit of massive clast-supported boulders and cobbles within a gravelly and sandy matrix (Gmc) where fragments of amphora were found and connected to the Roman Period (1st century CE). This deposit is interpreted to be representative of a phase of enhanced hydro-sedimentary activity. It is followed by a sandy deposit with gravel (Sm-G) and laminated sand and silt (Sh-Fl). Upwards, the clasts stacking in a fluvial active band deposit (Gmc-Gmm) suggested an apparent flow direction with the beginning of the progressive migration of the stream towards the northeast. It evolves into the three layers of silty sands classified as Sm, Sm-Fm and Sh-Fl where GIU_1–GIU_4 were sampled. They are attributed to a secondary fluvial channel and interpreted to be in layers of low river activity (Fig. 5c and Table 3). GIU_1 dated between 1170 and 1270 CE (Table 4) attests to the end of construction phases 1 and 2 and of the first phase of intense alluvial activity. GIU_2 dated from a hearth's remains found at the boundary between two layers has an age between 1260 and 1320 CE and is evidence of the last human activity for construction phases 1 and 2. GIU_3 collected below some building material provides the evidence of the beginning of construction phase 3 after 1460 CE. Construction phase 3 lasted until 1640 CE as shown by the age interval of sample GIU_4, found at the boundary before the deposition of the fluvial sediment Sh-Fl (Fig. 5c). Construction phase 3 was partially destroyed by some alluvial events that must have occurred after 1640 CE and before construction phase 4. An alluvial event characterised by a sandy deposit with pebbles and gravel (Sm) cuts all the previous layers including structures of construction phase 3 and a wall belonging to construction phase 4 (Fig. 5c). A sample of charcoal (Table 3, GIU_5) found within this sandy alluvial deposit allowed us to determine a radiocarbon age of the alluvial event between 1660 and 1950 CE, suggesting the occurrence of a phase of enhanced hydro-sedimentary activity after 1660 CE and before 1790 CE, the year of the construction of Villa Rusconi.
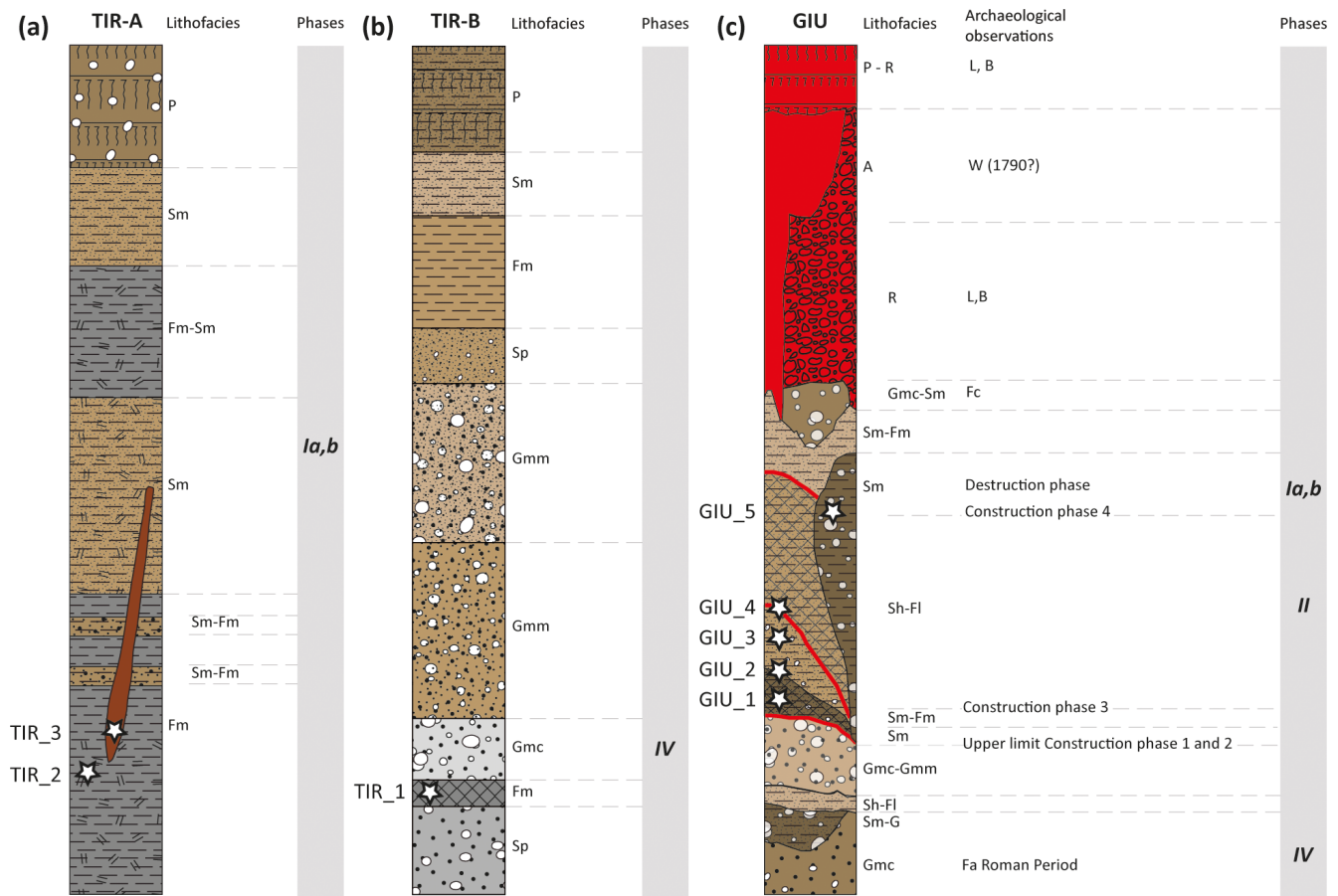
Figure 5. Stratigraphic logs in a timescale representation, with their corresponding lithofacies and archaeological remains. The phases (grey shaded) correspond to the enhanced hydro-sedimentary phases defined in Sect. 5.1. Sites: **(a)** Gaggiolo Lungo, Gudo (TIR-A; Scapozza et al., 2017); **(b)** Boschetti, Sementina (TIR-B; Scapozza et al., 2017); **(c)** Giubiasco, Palasio (GIU). Codes for archaeological observations: B = backfilling; Ffs = fragments of flint stone; Fp = fragments of pottery; L = levelling; Pv = pavement; W = wall.

The Giubiasco, Palasio, site provides the evidence of three events of enhanced hydro-sedimentary activity (Fig. 5c). The first is directly observed in the stratigraphic sequence and occurred during the Early and High Middle Ages. The second event must have occurred between construction phases 2 and 3 during the Late Middle Ages. The third and last event is associated with the destruction of construction phases 3 and 4 during the modern and contemporary periods.

4.2.6 Claro, Torrazza (TOR)

The field observations for the site Claro, Torrazza (Fig. 1, TOR), were resumed in a representative stratigraphic sequence that counts 10 units of natural deposits. No archaeological evidence is presented for this particular section (Fig. 6a).

The Gmm unit at the bottom of the sequence is characterised as a hyperconcentrated deposit (Gmm). Afterwards, four more levels suggesting a higher energy of sedimentary transport were observed and described as Gmc, Sl, Gmc,

Gmc (-Gmm), Sm-Sl and Gmc just below the superficial soil layer. The coarse-grained levels are alternated with some sandy silts (Fm), from which four samples of charcoal were collected for radiocarbon dating (Fig. 6a and Table 3).

The results indicate a range of ages between 3530 BCE (TOR_1) and 120 CE (TOR_4, Table 4), covering a period including the Neolithic, the Bronze Age and the Iron Age. The four phases of enhanced hydro-sedimentary activity observed in TOR have possibly occurred in this interval of time. The radiocarbon ages are coherent with the human settlements of the Iron Age observed in others sectors of the studied site (Cardani Vergani, 2020).

4.2.7 Claro (CLA)

The observations for Claro (Fig. 1, CLA) were resumed in two stratigraphic sequences according to the different areas: CLA-L for "Longo" and CLA-R for "In Rasaréi".

The stratigraphy of CLA-L (Fig. 6b) presents eight units of natural fluvial deposits. The sequence starts with two units
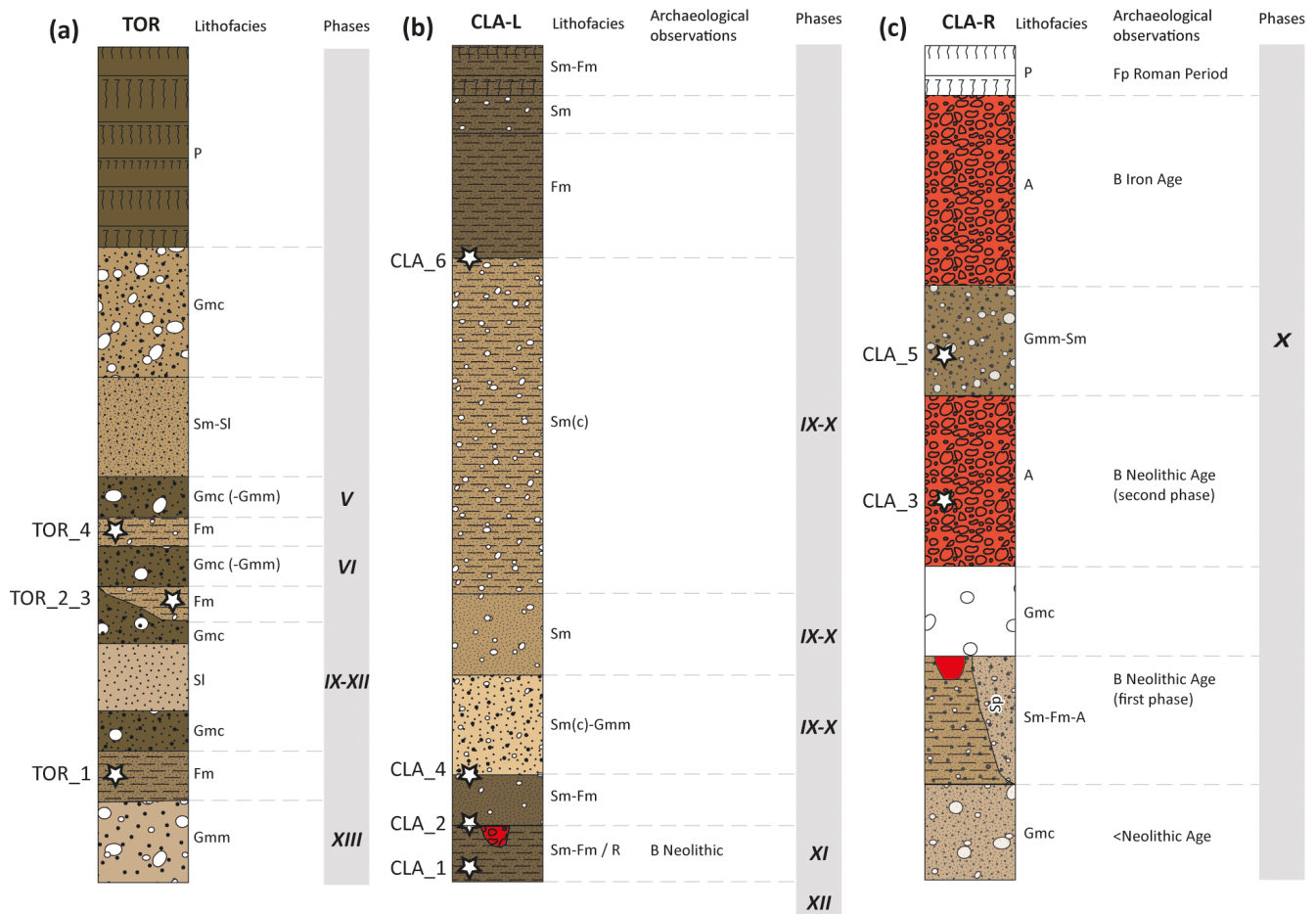
Figure 6. Stratigraphic logs in a timescale representation, with their corresponding lithofacies and archaeological remains. The phases (grey shaded) correspond to the enhanced hydro-sedimentary phases defined in Sect. 5.1. Sites: **(a)** Claro, Torrazza (TOR); **(b)** Claro, Longo (CLA-L); **(c)** Claro, In Rasaréi (CLA-R). Codes for archaeological observations: B = backfilling; Fp = fragments of pottery.

consisting of layers of fine silty sand (Sm-Fm) and attributed to palaeosoils. Between the two units some remnants of anthropic structures, such as backfillings, were observed. Those were buried by the deposits of the second unit, which suggests a phase of intense alluvial activity affecting the settlements of the Neolithic Age. Afterwards three units of alluvial deposits of low to medium energy were described: the Sm(c)-Gmm unit which consists of a filling deposit of the fluvial channel and the overlaying poorly graded sands with gravel, Sm and Sm(c), which were probably formed by rapid decantation during the final part of the solid transport after depositing the coarser material. At the top of the sequence three units of fine sediments more or less rich in silt showed a partial or advanced pedogenesis (Fm, Sm or Sm-Fm).

Two phases of more intense alluvial activity described for CLA-L were constrained by radiocarbon dating on four charcoal samples (Fig. 6b and Table 3). A first phase during the Neolithic lasted until 2680 BCE (lower limit of the interval of ages determined for CLA_2, Table 4), and subsequently a second phase must have occurred between 2340 BCE and

820 BCE (upper limit of ages for sample CLA_4 and lower limit of ages for sample CLA_6, Table 4).

In the case of CLA-R, the stratigraphic sequence shows eight different units, of which five are natural deposits and three are of anthropic origin (Fig. 6c), described as a first Neolithic phase, a second Neolithic phase and an Iron Age phase (Cardani Vergani, 2019, 2020, 2021). The bottom of the sequence consists of a coarse deposit attributed to an active fluvial band (Gmc), followed by a finer layer of a low-transport-energy fluvial deposit with some silt (Sm-Fm), which laterally varies in a planar crossbedded sandy deposit (Sp), and with evidence of trenches and backfillings attributed to the first Neolithic phase. Towards the top, a layer issued by a hyperconcentrated deposit (Gmm) was observed. Between the two backfillings of Neolithic and Iron Age, an alluvial deposit unit classified as Gmm-Sm was described and interpreted as a more intense alluvial activity phase. A unit characterised as actual soil was observed at the top of the stratigraphic sequence, but the findings of pottery fragments of the Roman Period indicate that it is actually older.
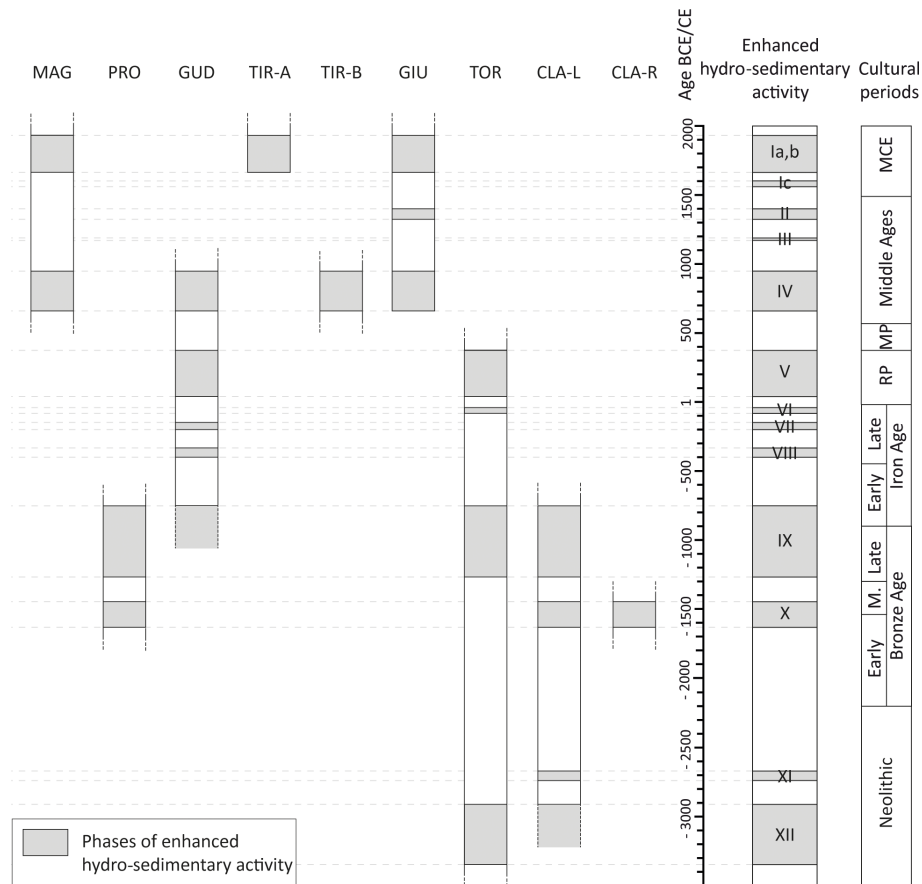
Figure 7. Synthetic representation of the enhanced hydro-sedimentary phases of the Ticino river based on the nine study sites in relation to the chronology of the cultural periods for the southern Swiss Alps. The sites are listed from the west to the east as presented in Fig. 1. The intervals of ages of each phase are shown in Table 5, and the cultural periods are described in Table 2.

In CLA-R two samples of charcoal were collected for radiocarbon dating (Fig. 6c and Table 3): the results for sample CLA_3 (2520 BCE, median calibrated age in Table 4) attribute it to the Neolithic Age, whereas the radiocarbon ages for sample CLA_5 constrain the enhanced hydrosedimentary activity phase observed between 1620 and 1450 BCE (Table 4), attributed to the Bronze Age. Both radiocarbon dating results are coherent with the archaeological observations.

5 Discussion

5.1 Interpretation of the phases of enhanced hydro-sedimentary activity

The joint analysis of the lithostratigraphy and archaeological evidence of anthropic artefacts and settlements allowed for the definition of 13 phases of enhanced hydro-sedimentary activity in the Ticino river and its tributaries since the Neolithic (Table 5 and Fig. 7). Several phases were recognised in both the Ticino river and stream tributaries (phases Ia, Ib, Ic and IV), as well as other phases in more than one site

(phases Ia, Ib, IV, V, IX, X and XII), whereas some phases were described only at one site (phases II, VI, VII, VIII, XI and XIII). Only phase III, related to the flood of 1178 CE, was defined exclusively from historical sources (Scapozza, 2013). Differences in age constraint through time allow us to define decadal to secular phases (phases I, II, VI, VII, VIII, X and XI), such as longer multi-secular phases (phases IV, V, IX and XII). With the exception of the single event defined by phase III, the length of historic phases is between 35 (phase Ic) and 360 years (phase V), whereas for protohistoric and prehistoric phases it is between 30 (phases VII and VIII) and 520 years (phase IX).

Phases of the contemporary and modern periods, as well as of the Middle Ages, were defined thanks to the joint analysis of historical sources (Scapozza, 2013), fluvial deposit stratigraphy in the Ticino river floodplain (Scapozza and Oppizzi, 2013; Scapozza et al., 2017) and geoarchaeological observations carried out on the site of Giubiasco, Palasio (GIU). A period of intense fluvial activity during the second half of 17th century, the 18th and 19th centuries, and the first half of 20th century was recognised on the Ticino

Table 5. Phases of enhanced hydro-sedimentary activity constrained with radiocarbon dating of samples of the present study, previous research and historical data. For the precise interval of ages corresponding to the source sample, see Table 4. For the detailed chronology for the cultural periods, see Table 2.

Phases	Cultural period	Start of the phase (BCE/CE)	End of the phase (BCE/CE)	Source
Ia	Contemporary period	1868	1930	Scapozza (2013)
Ib	Modern and contemporary periods	1777	1840	Scapozza (2013)
Ia, b	Modern and contemporary periods	1680	1930	TIR_3
Ia, b	Modern and contemporary periods	1690	1920	MAG_3
Ia, b	Modern and contemporary periods	1660	1820	GIU_5, archeological interpretation
Ic	Modern period	1566	1601	Scapozza (2013)
II	Late Middle Ages	1320	1400	GIU_2, GIU_3
III	High Middle Ages	1178	1178	Scapozza (2013), Scapozza and Oppizzi (2013)
IV	Early Middle Ages/High Middle Ages	6th and 7th centuries	< 1170	Archaeological interpretation, GIU_1
IV	Early Middle Ages	680	960	MAG_2, MAG_1
IV	Early Middle Ages	680–890		TIR_1
IV		> 550		GUD_5
V		< 120		TOR_4
V	Roman Period	20	380	GUD_4, GUD_5
VI			< −60	TOR_4
VII	La Tène C (Late Iron Age)	−200	−170	GUD_2, GUD_4
VIII	La Tène B (Late Iron Age)	−400	−370	GUD_1, GUD_3
IX		> −800		TOR_2, TOR_3
IX			< −910	TOR_2, TOR_3
IX	Late Bronze Age/Early Iron Age	−1280	−760	PRO_1, GUD_1
X	Middle Bronze Age	−1620	−1450	CLA_5, PRO_1
IX–X		−2340	−820	CLA_4, CLA_6
XI	Neolithic	−2750	−2680	CLA_1, CLA_2
XII	Neolithic	−3360	−2920	TOR_1, CLA_1
XIII	Neolithic		< −3530	TOR_1

river delta between 1690 and 1920 CE (MAG_3), on the Ticino river floodplain between 1680 and 1930 CE (TIR_3), and in the stream of Giubiasco, Palasio, between 1660 and 1820 CE (GIU_5 and archaeological evidence). Evidence for phase IV occurring during the Early Middle Ages was also found in several locations. On the Ticino river delta, this phase was dated between 680 and 960 CE (MAG_1 and MAG_2), whereas observations collected on the floodplain have provided a dating after 680–890 CE (TIR_1). Partial evidence from Gudo indicates a beginning of this phase after 550 CE (GUD_5), whereas archaeological attribution of a building and radiocarbon dating of GIU_1 from Giubiasco, Palasio, indicate a phase of activity of tributary streams that began during the 6th/7th century CE and ended before 1170 CE.

For the Roman Period, the Iron Age and the Bronze Age, the six phases of enhanced hydro-sedimentary activity (one during the Roman Period, three during the Iron Age and two during the Bronze Age) were defined thanks to complementary evidence from the two sites of Claro (CLA-R and TOR) and the two sites of Gudo (GUD and PRO). For phase IX, the starting and ending dates (1280 and 760 BCE) were defined clearly thanks to the complementary stratigraphy of the two sites of Gudo (dating PRO_1 and GUD_1). A coherent result was defined thanks to observations from Claro, Torrazza, where an antecedent phase was defined as ending before 910 BCE, and a subsequent phase was defined as beginning after 800 BCE (TOR_2 and TOR_3). Phase X occurred during the Early and Middle Bronze Age and was defined thanks to a hyperconcentrated deposit dated between 1620 and 1490 BCE in Claro (CLA_5) and was

also recognised, with similar sedimentological evidence, in Gudo, Progero (PRO_1). The three phases of the Neolithic were finally defined thanks to the three sites investigated in Claro (CLA-L, CLA-R and TOR), for which lithostratigraphical complementarity allowed us to define phase XII according to the terminus post quem (3360 BCE) defined by TOR_1 and the terminus ante quem (2920 BCE) defined by CLA_1.

5.2 Palaeoenvironmental and palaeoclimatic causes of the enhanced hydro-sedimentary activity phases

5.2.1 Neolithic and Early Bronze Age (5500–1550 BCE)

Phase XIII (> 3530 BCE) occurred before and during the beginning of the Piora II cold climate oscillation (ca. 3550–3000 BCE according to a new calibration of period dating from Burga et al., 2001), whereas phase XII (3360–2920 BCE) occurred during/just after this climate oscillation. Considering also phase XI (2750–2680 BCE), the three enhanced hydro-sedimentary activity phases evidenced during the Neolithic occurred during periods of general glacier recession in the Swiss Alps, which were dated between 3710–3540 and 3340–1920 BCE (Hormes et al., 2006) and 3750–3550 and 3250–2450 BCE (Joerin et al., 2006). These three phases also correspond to minor peaks of flood activity on the southern side of the Alps, defined thanks to the analysis and dating of lacustrine sediments in southern Switzerland and northern Italy (Wirth et al., 2013). Phase XII ended in agreement with the lowest residual Δ^{14}C values recorded between 3000 and 450 BCE (Fig. 8), with the negative peak (minimal value of −10.6‰ in 2935 BCE) indicating high solar activity. On the contrary, the period between phases XII and XI was characterised by very low solar activity, as indicated by the positive peak presenting the highest maximal value (+16.1‰ in 2825 BCE) of the last 5000 years (Fig. 8). No evidence of enhanced river activity was observed for more than a millennium between 2680 and 1620 BCE even if in Claro a long sequence of coarse fluvial sediments, assuming several phases of hydro-sedimentary activity, was dated between 2340 BCE (CLA_4) and 820 BCE (CLA_6) (Table 5). Those phases correspond to the period of enhanced rainfall evidenced by Wirth et al. (2013) between 2250 and 450 BCE (Fig. 8).

Palynological evidence from the peat bog of Guér, located above Claro (coord. CH1903+/LV95: 2 722 050/1 126 500; 835 m a.s.l.), indicates a progressive increase in the anthropic pressure on the territory during the Neolithic, supported by the numerous archaeological investigations carried out in Claro and neighbouring localities (Morales-Molino et al., 2015; Carlevaro et al., 2017). Cultural indicators (CIs; sum of Cerealia-type and *Plantago-lanceolata*-type pollen; Tinner et al., 2003) and microscopic charcoal concentration indicate an increase in anthropic pressure between 3300 and 2600 BCE (Morales-Molino et al., 2015), which reached a peak between 2500 and 1850 BCE as indicated also by the

maximum values of fire frequency episodes of the Neolithic and Early Bronze Age (Fig. 8).

5.2.2 Middle and Late Bronze Age and Iron Age (1550–15 BCE)

Phases X (1620–1490 BCE) and IX (1280–760 BCE) occurred during the period of enhanced rainfall of the beginning of the Meghalayan Stage/Age (Fig. 8). Phase X, in particular, occurred during a cold and moist climate phase (1650–1450 BCE; Tinner et al., 2003) of the Löbben cold climate oscillation (ca. 1800–1350 BCE; Burga et al., 2001), which characterised the transition from the Early to the Middle Bronze Age (Fig. 8). Phase IX, on the contrary, corresponds almost entirely with the warm and dry climate of the Bronze Warm Period (ca. 1350–950 BCE), which was intercalated between the Löbben and Göschenen I cold climate oscillations (Burga et al., 2001).

The period of enhanced rainfall ending in the Early Iron Age was characterised, around 550 BCE, by the highest flood activity recorded in the southern Alps for the entire Holocene (Wirth et al., 2013; Fig. 8). This peak was synchronous with the maximum Grosser Aletschgletscher (Great Aletsch Glacier) advance of 1000–600 BCE (Holzhauser et al., 2005) corresponding to the Göschenen I cold climate oscillation (ca. 950–300 BCE; Burga et al., 2001). After the intense rainfall period, three well-constrained enhanced hydro-sedimentary phases were defined during the Late Iron Age. Phase VIII (400–370 BCE) occurred after the lowest peak in residual Δ^{14}C values (minimal value of −11.7‰ in 420 BCE) ever recorded between 3000 BCE and 1100 CE. Phase VII (200–170 BCE), corresponding to a secondary peak of the flood activity on the southern side of the Alps, occurred during a cold and moist climate phase (225–175 BCE; Tinner et al., 2003) at the beginning of the Roman Warm Period (300 BCE–400 CE; Patterson et al., 2010). Together with phase VI (ending before 60 BCE but whose beginning was not determined), they occurred during the generalised glacier retreat period of the Roman Warm Period, dated between 350 BCE and 780 CE (Hormes et al., 2006) and between 200 BCE and 100 CE (Joerin et al., 2006).

The period between phases IX and VII was characterised, on the lower part of the slopes of the Ticino Valley, by a significant intensification of land use during the Early Iron Age and the beginning of Late Iron Age (Tinner et al., 2003; Morales-Molino et al., 2015; Carlevaro et al., 2017). Evidence from the Guér peat bog indicates a peak of microscopic charcoal concentration around 650 BCE, with the maximum frequency of fire episodes (more than eight episodes per thousand years; see Fig. 8) registered between 900 and 300 BCE. Pollen used as CIs presented, during this period, a maximum peak around 800 BCE for the *Plantago lanceolata* type and around 300 BCE for the Cerealia type (Morales-Molino et al., 2015). The link between indicators for fire episodes and CI, as well as the presence of several archae-
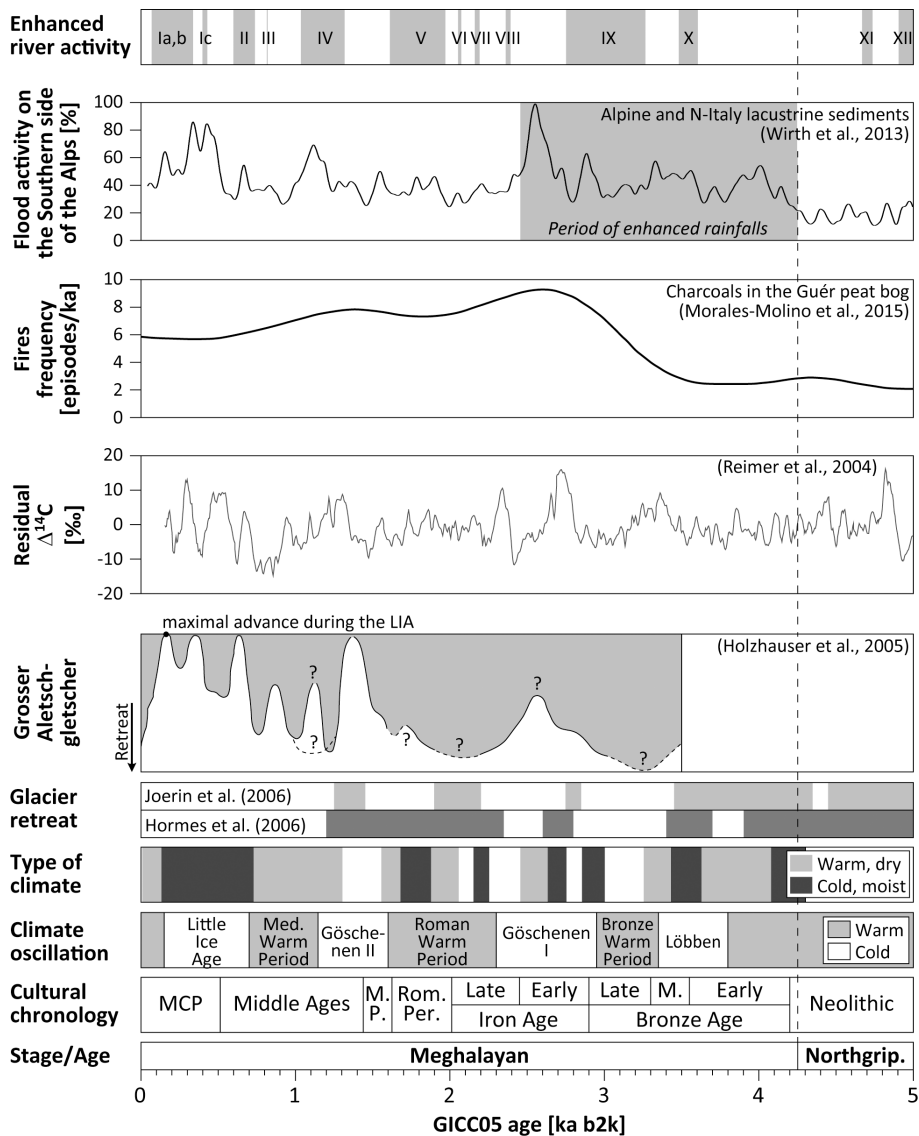
Figure 8. Enhanced river activity phases defined in this study, compared with the main morphoclimatic indicators defined for the central and southern Swiss Alps during the Meghalayan Stage/Age (Upper/Late Holocene subseries/subepoch) compiled by Scapozza (2019). Sources: type of climate from Tinner et al. (2003) for the period between 2300 BCE and 800 CE, from Mann et al. (2009) for the Medieval Warm Period, and from Zumbühl and Holzhauser (1988) for the Little Ice Age; climate oscillations from Burga et al. (2001), as well as from Patterson et al. (2010) for the Roman Warm Period; cultural chronology from Table 3. Abbreviations: GICC05 = Greenland Ice Core Chronology 2005; LIA = Little Ice Age; M. = middle; MCP = modern and contemporary period; M. P. = Migration Period; Northgrip. = Northgrippian; Rom. Per. = Roman Period.

ological sites in Claro and neighbouring localities during the Bronze Age and the Iron Age, indicates significant human-controlled fire activity during this period (Morales-Molino et al., 2015; Carlevaro et al., 2017). Despite the reduced forest cover and the period of climatic degradation corresponding to Göschenen I oscillations, less evidence for enhanced hydro-sedimentary activity can be obtained from archaeological sites. As highlighted by the L-shaped wall discovered in Gudo, erected in the period 370 and 200 BCE between phases VIII and VII of enhanced hydro-sedimentary activity, it is

probably during the Iron Age that there was a stabilisation of human settlements which led to the need to build dams to contain water coming from the valley bottom river and/or from streams on the slope (Scapozza and Czerski, 2019).

5.2.3 Roman Period and Middle Ages (15 BCE–1492 CE)

Phase V (20–380 CE) occurred during the Roman Period corresponding to the cold and moist climate phase of 150–
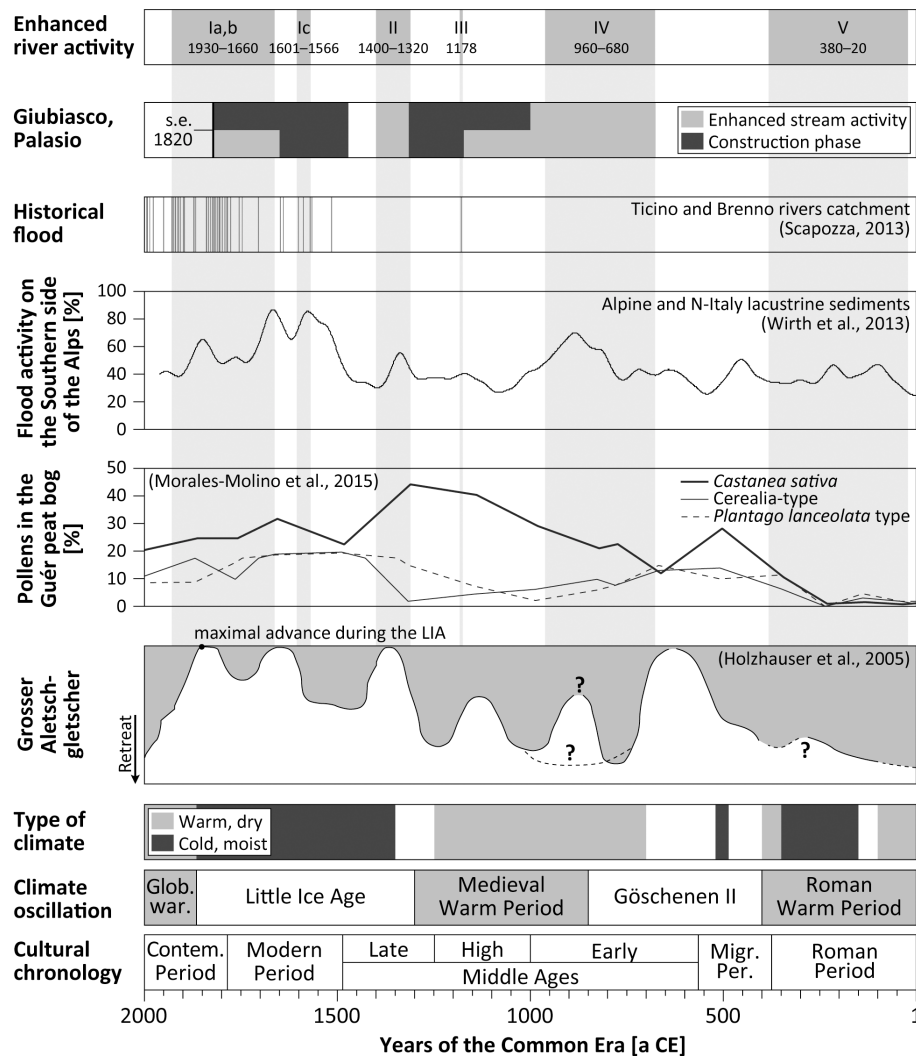
Figure 9. Enhanced river activity phases and construction phases for Giubiasco, Palasio (GIU), defined in the study, compared with the main morphoclimatic indicators defined for the central and southern Swiss Alps during the common era. Sources: see Fig. 8. Abbreviations: Contem. = contemporary; Glob. war. = global warming; LIA = Little Ice Age; Migr. Per. = Migration Period; s. e. = stream embankment.

350 CE (Tinner et al., 2003), placed in the Roman Warm Period (Fig. 9). Phase IV (680–960 CE), occurred between the Göschenen II cold climate oscillation (400–850 CE; Burga et al., 2001) and the Medieval Warm Period (850–1300 CE; Mann et al., 2009), mainly corresponding to the warm and dry climate phase of 700–1250 CE (Tinner et al., 2003; Mann et al., 2009). Within this phase is placed the peak of flood activity culminating around 900 CE (Wirth et al., 2013; Fig. 9). The period between phases V and IV (380–680 CE) was marked by the first peak in *Castanea sativa* pollen in 510 CE after the introduction and cultivation of this tree species around 150 CE (Morales-Molino et al., 2015). Frequency of fire episodes, after a second-order minimum in the first centuries of the common era, presents the second highest peak (just below eight episodes per thousand years; see Fig. 8) between 400 and 800 CE, indicating an increased anthropic pressure during the Migration Period and the Early Middle Ages (Morales-Molino et al., 2015).

Phase V, which was defined thanks to evidence from valley side streams in Claro, Torrazza (TOR_4), and Gudo (GUD_4 and GUD_5; Table 5), has not been recognised in the Ticino river, which rather presented a particularly calm period of hydro-sedimentary activity during the Roman Period and the Migration Period (Scapozza and Oppizzi, 2013). Phase IV, on the contrary, perfectly corresponds to the period of enhanced hydro-sedimentary activity evidenced both on the Ticino river floodplain (Scapozza and Oppizzi, 2013; Scapozza et al., 2017) and in the valley side streams of Giubiasco and Gudo. The multiplication of evidence for this phase indicated that it was generalised on the southern side of the Alps. It was also recognised in the French Upper Rhone catchment (Haut Rhône) where, after repeated heavy rain episodes be-

tween 100 BCE and 100 CE, followed by rare flood events between 100 and 250 CE and a relatively dry period between 250 and 500 CE (Bravard et al., 1992; Arnaud et al., 2005), the three centuries between 500 and 800 CE were marked by a phase of moderate torrential activity and by a significant resumption of river activity (Arnaud-Fassetta and Landuré, 2003; Arnaud et al., 2005; Salvador et al., 2005).

Phase III (1178 CE) occurred during the Medieval Warm Period after almost two centuries of low hydrological activity and, as already mentioned in Sect. 5.1, was defined only on the basis of historical information (Scapozza, 2013). Based on a single flood episode, this phase cannot be correlated with a specific phase of enhanced hydro-sedimentary activity. Considering that on the French Upper Rhone the main phases are probably slightly older than on the Ticino river (Scapozza and Oppizzi, 2013), this period of low activity corresponds with the phase of deficient hydrology of 800–1000 CE and/or the phase of rare erosive events of 1000–1100 CE (with the lowest hydrological index of 0 and 1, respectively, on a scale of 5) defined by Bravard et al. (1992) and affirmed by Arnaud et al. (2005). Flood events were recognised on the Upper Rhone River between 1050 and 1250 CE (Bravard et al., 1992; Arnaud et al., 2005), indicating that the 1178 CE flood on the Ticino river may not have been the only one in that period. Between phases IV and III, in Giubiasco the first Medieval phase of construction (11th–12th centuries) was identified, ending before 1170 CE (GIU_1, Table 4). A second construction phase was identified between 1170 and 1320 CE, i.e. before phase II of enhanced hydrological activity, dated between 1320 and 1400 CE (GIU_2 and GIU_3), which destroyed the building erected during the first two Medieval construction phases.

Phase II (1320–1400 CE) presents a very good correspondence with the period of increased flood activity on the southern side of the Alps evidenced between 1300 and 1400 CE (Wirth et al., 2013; Fig. 9) and corresponding to the first phase of the Little Ice Age, which is characterised by glacier advance between 1300 and 1350 CE (Holzhauser et al., 2005). This phase occurred just after the peak of *Castanea sativa* pollen recorded in Guér, above Claro, around 1300 CE (Fig. 9), belonging to the second maximum of sweet chestnut of 1150–1450 CE caused by its flourishing use for staple food production and characterised by the highest pollen concentrations since the chestnut introduction in 150 CE (Morales-Molino et al., 2015).

5.2.4 Modern and contemporary periods (1492 CE–today)

Phase I corresponds with the generalised hydro-sedimentary rupture characterising the period between the 16th and 19th centuries which is related to the coldest phases of the Little Ice Age (Pfister, 1984; Zumbühl and Holzhauser, 1988; Scapozza, 2014) and defined as a "major torrential

crisis" in the French Upper Rhone River, with a hydrological index of 5/5 between 1350 and 1800 CE (Bravard et al., 1992; Arnaud et al., 2005). Considering the historical flood events compiled for the Swiss Ticino river catchment, with 38 flood events identified between 1566 and 1930 CE (Scapozza, 2013:81; Fig. 9), phase I can be divided into three sub-phases of major flood frequency (> 10 events per 100 a): phase Ic, with 5 floods between 1566 and 1601 CE (14 events per 100 a); phase Ib, with 16 floods between 1777 and 1840 CE (25 events per 100 a), and phase Ia, with 12 floods between 1868 and 1930 CE (19 events per 100 a). Considering also the field evidence for these phases of major river activity, coming from the Ticino river delta (MAG_3 in Table 4; Scapozza and Oppizzi, 2013), the Ticino river floodplain (TIR_3; Scapozza et al., 2017) and the site of Giubiasco (GIU_3), phases Ia and Ib were grouped and cover the period between 1660 and 1930 CE (Table 5). Especially in Giubiasco, the structures built during construction phase 3 (corresponding to the 1470–1640 CE period of hydro-sedimentary calm) were destroyed between 1660 and 1790 CE. The enhanced torrential activity ended only in 1820 CE following the embankment of the stream.

6 Conclusion

Three main conclusions can be drawn from the lithostratigraphical observations and the geochronological assessments thanks to radiocarbon dating and archaeological interpretations at the study sites:

1. The combined approach allowed us to determine 13 phases of enhanced hydro-sedimentary activity of the Ticino river and its tributaries since the Neolithic. The three phases of the Neolithic (XIII, XII, XI) were defined thanks to the three sites investigated in Claro (CLA-L, CLA-R and TOR). The phases for the Bronze Age (X, IX), the Iron Age (IX, VIII and VII) and the Roman Period (V) were defined thanks to complementary evidence both from the two sites of Claro (CLA-R and TOR) and from the two sites of Gudo (GUD and PRO). Phases of the Middle Ages (IV, III and II), as well as of the modern and contemporary periods (Ic, Ia, b, Ib and Ia), were defined thanks to the joint analysis of historical sources, fluvial deposit stratigraphy in the Ticino river floodplain and geoarchaeological observations carried out on the site of Giubiasco, Palasio (GIU).

2. The phases of enhanced hydro-sedimentary activity could be linked to regional or continental palaeoenvironmental and palaeoclimatic causes. In fact, most of them were observed in concurrence with periods of climate degradation with the establishment of cold and humid conditions, supported by data of glacier fluctuations in the Swiss Alps and/or by the increase in flood activity on the southern side of the Alps. Among these

phases are included the phase X of the Middle Bronze Age, phase IX of the Late Bronze Age/Early Iron Age, phases VIII and VII of the Late Iron Age, phase V of the Roman Period, phase IV of the Early Middle Ages and all the events related to phases II and I that occurred between the Late Middle Ages and the contemporary period. Phases II and I in particular are related to the last cold climate oscillation of the Little Ice Age.

3. The collected data allowed us to assess the impacts of these increased alluvial phases on the human communities and to confirm some of the sedimentological and archaeological observations from the field. In the archaeological site of Gudo (GUD), for example, the construction of an L-shaped wall, erected in the period 370–200 BCE between phases VIII and VII of enhanced hydro-sedimentary activity, proved the need to build dams to contain water coming from the valley bottom river and/or from streams on the slope. Also in Giubiasco, Palasio (GIU), the torrential events attributed to the Little Ice Age climate oscillation had a strong impact on the construction and destruction phases observed.

All the results confirmed the validity of the combined approach applied in this study. In the future, the overview on the evolution of the morphosedimentary dynamics of the Ticino river and its tributaries presented herein will be continuously refined and updated with further sedimentological and archaeological observations.

References

Académies suisses des sciences: Coup de projecteur sur le climat suisse, Etat des lieux et perspectives, swiss academies reports, 11/5, p. 218, available at: https://proclim.scnat.ch/fr/activities/brennpunkt/downloads (last access: 21 December 2021), 2016.

Arnaud, F., Revel, M., Chapron, E., Desmet, M., and Tribovillard, N.: 7200 years of Rhône river flooding activity in Lake Le Bourget, France: a high-resolution sediment record of NW Alps hydrology, Holocene, 15, 420–428, https://doi.org/10.1191/0959683605hl801rp, 2005.

Arnaud-Fassetta, G., and Landuré, C.: Hydroclimatic hazards, vulnerability of societies and fluvial risk in the Rhône Delta (Mediterranean France) from the Greek period to the Early Middle Ages, in: The Mediterranean World Environment and History, Proceedings of the International Conference "Environmental Dynamics and History in Mediterranean Areas" held in Paris, 24–26 April 2002, edited by: Fouache E., Elsevier, Paris, France, 51–76, 2003.

Bravard, J. P. and Petts, G. E.: Human impacts on fluvial systems, in: Fluvial hydrosystems, edited by: Petts, G. E. and Amoros, C., Chapman & Hall, London, UK, 233–256, 1996.

Bravard, J.-P., Verot-Bourrely, A., and Salvador, P.-G.: Le climat d'après les informations fournies par les enregistrements sédimentaires fluviatiles étudiées sur des sites archéologiques, Les nouvelles de l'Archéologie, 50, 7–14, 1992.

Bronk Ramsey, C.: Development of the Radiocarbon Program OxCal, Radiocarbon, 43, 355–363, https://doi.org/10.1017/S0033822200038212, 2001.

Bronk Ramsey, C.: OxCal 4.4 Manual, Radiocarbon Accelerator Unit, Oxford, United Kingdom, available at: https://c14.arch.ox.ac.uk/oxcal/OxCal.html (last access: 21 December 2021), 2020.

Burga, C., Perret, R., and Zoller, H.: Swiss localities of early recognized Holocene climate oscillations – characterisation and significance, Vier. Natur. Gesell. Zürich, 146, 65–74, 2001.

Cailleux, A. and Tricart, J.: Initiation à l'étude des sables et des galets, 3 vol., Centre de Documentation Universitaire, Paris, France, 1963.

Cardani Vergani, R.: Ricerche archeologiche in Cantone Ticino nel 2017, Boll. Ass. Archeol. Ticin., 30, 30–37, https://doi.org/10.5169/seals-737980, 2018.

Cardani Vergani, R.: Ricerche archeologiche in Cantone Ticino nel 2018, Boll. Ass. Archeol. Ticin., 31, 21–35, 2019.

Cardani Vergani, R.: Ricerche archeologiche in Cantone Ticino nel 2019, Boll. Ass. Archeol. Ticin., 32, 26–33, 2020.

Cardani Vergani, R.: Ricerche archeologiche in Cantone Ticino nel 2020, Boll. Ass. Archeol. Ticin., 33, 24–31, 2021.

Carlevaro, E.: Dinamiche del popolamento nell'area sudalpina dal Bronzo finale alla romanizzazione, Università di Zurigo, Zurigo, Svizzera, 343 pp., available at: https://zora.uzh.ch/id/eprint/164250/ (last access: 21 December 2021), 2013.

Carlevaro, E., Colombaroli, D., Conedera, M., Krebs, P., Morales-Molino, C., Scapozza, C., Tinner, W., and Vescovi, E.: Claro e il suo territorio, Archeol. Schweiz, 40, 24–29, https://doi.org/10.5169/seals-768568, 2017.

Conedera, M. and Tinner, W.: Ferro e fuoco: una ricostruzione paleoecologica dell'approccio territoriale nella Regione Insubrica in età preistorica, in: I Leponti, tra mito e realtà, edited by: de Marinis, R. C. and Biaggio Simona, S., Armando Dadò, Locarno, Svizzera, 63–70, 2000.

Crivelli, A.: Atlante preistorico e storico della Svizzera italiana, Ristampa anastatica dell'edizione del 1943 e aggiornamento a cura di P. A. Donati, Casagrande, Bellinzona, Svizzera, p. 156, 1990.

De Marinis, R. C. and Biaggio Simona, S.: I Leponti, tra mito e realtà, 2 vol., Armando Dadò, Locarno, Svizzera, 419 + 489 pp., 2000.

Documentazione IVS Cantone Ticino: Percorso TI 1.2.3: Strada francesca (sponda sinistra), Bellinzona/Ravecchia – Giubiasco, Inventario delle vie di comunicazione storiche della Svizzera (IVS)m Bern, Schweiz, p. 2, 1999.

Donati, P.: Bellinzona a Castel Grande: 6000 anni di storia, Archeol. Schweiz, 9, 94–109, https://doi.org/10.5169/seals-8233, 1986.

Glaser, R., Ammann, B., Brauer, A., Heiri, O., Jacobeit, J., Lotter, A. F., Luterbacher, J., Maisch, M., Magny, M., Pfister, C., Tinner, W., Veit, H., and Wanner, H.: Palaeoclimate within the River Rhine Catchment during Holocene and Historic Times, Erdkunde, 59, 251–275, 2005.

Grant, J., Gorin, S., and Fleming, N.: The archaeology coursebook: an introduction to study skills, topics and methods, Routledge, London, UK, p. 692, 2015.

Grossi, P.: Vita di un fiume. Consorzio correzione fiume Ticino dalla Moesa al Lago Maggiore 1886–1986, Salvioni, Bellinzona, Svizzera, 395 pp., 1986.

Holzhauser, H., Magny, M., and Zumbühl, H. J.: Glacier and lake-level variations in west-central Europe over the last 3500 years, Holocene, 16, 789–801, https://doi.org/10.1191/0959683605hl853ra, 2005.

Hormes, A., Beer, J., and Schlüchter, C.: A geochronological approach to understanding the role of solar activity on Holocene glacier length variability in the Swiss Alps, Geogr. Ann. A, 88, 282–294, https://doi.org/10.1111/j.0435-3676.2006.00301.x, 2006.

James, L. A. and Marcus, W. A.: The human role in changing fluvial systems: Retrospect, inventory and prospect, Geomorphology, 79, 152–171, https://doi.org/10.1016/j.geomorph.2006.06.017, 2006.

Joerin, U. E., Stocker, T. F., and Schlüchter, C.: Multicentury glacier fluctuations in the Swiss Alps during the Holocene, Holocene, 16, 697–704, https://doi.org/10.1191/0959683606hl964rp, 2006.

King, C. A.: Techniques in geomorphology, Arnold, London, UK, p. 342, 1966.

Laigre, L., Reynard, E., Arnaud-Fassetta, G., Baron, L., and Glenz, D.: Caractérisation de la paléodynamique du Rhône en amont de Martigny (Valais, Suisse) à l'aide de la tomographie de résistivité électrique (TRE), Géomorphologie, 4, 405–426, https://doi.org/10.4000/geomorphologie.10020, 2012.

Mann, M. E., Zhang, Z., Rutherford, S., Bradley R. S., Hughes, M. K., Shindell, D., Ammann, C., Faluvegi, G., and Fenbiao, N.: Global signatures and dynamical origins of the Little Ice Age and Medieval Climate Anomaly, Science, 326, 1256–1260, https://doi.org/10.1126/science.1177303, 2009.

Martinoli, G.: La correzione del fiume Ticino dal riale di Sementina al Lago Maggiore, Benzinger & Co., Einsiedeln, Svizzera, p. 63, 1896.

Miall, A. D.: A review of the braided river depositional environments, Earth Sci. Rev., 13, 1–62, https://doi.org/10.1016/0012-8252(77)90055-1, 1977a.

Miall, A. D.: Lithofacies types and vertical profile models in braided river deposits: a summary, in: Fluvial Sedimentology, edited by: Miall, A. D., Geological Survey of Canada, Calgary, Canada, 597–604, 1977b.

Minor, H.-E., Hager, W. H., Filippini, L., Pellandini, S., and Gheri-Pusch, A.: Ingegneria fluviale in Svizzera: sviluppo e prospettive, Società dell'arte e dell'ingegneria civile, Zurigo, Svizzera, p. 140, 2004.

Morales-Molino, C., Vescovi, E., Krebs, P., Carlevaro, E., Kaltenrieder, P., Conedera, M., Tinner, W., and Colombaroli D.: The role of human-induced fire and sweet chestnut (Castanea sativa Mill.) cultivation on the long-term landscape dynamics of the Southern Swiss Alps, Holocene, 25, 482–494, https://doi.org/10.1177/0959683614561884, 2015.

Moscato, S. (Ed.): Treccani 2000 Il mondo dell'archeologia, Vol. 1, Istituto della Enciclopedia Italiana, Roma, Italia, p. 1906, 2002.

Patterson, W. P., Dietrich, K. A., Holmden, C., and Andrews, J. T.: Two Millennia of North Atlantic seasonality and implications for Norse colonies, P. Natl. Acad. Sci. USA, 107, 5306–5310, https://doi.org/10.1073/pnas.0902522107, 2010.

Pfister, C.: Klimageschichte der Schweiz 1525–1860. Das Klima der Schweiz von 1525–1860 und seine Bedeutung in der Geschichte von Bevölkerung und Landwirtschaft, 2 Bd., Haupt, Bern, Schweiz, 245 + 174 pp., 1984.

Piffaretti, P. and Luchessa, C.: Lo scorrere del fiume, l'opera dell'uomo. 125 anni di attività del Consorzio Correzione Fiume Ticino (1886–2011), Salvioni, Bellinzona, Svizzera, 164 pp., 2011.

Reimer, P. J., Austin, W. E. N., Bard, E., Bayliss, A., Blackwell, P. G., Bronk Ramsey, C., Butzin, M., Cheng, H., Edwards, R. L., Friedrich, M., Grootes, P. M., Guilderson, T. P., Hajdas, I., Heaton, T. J., Hogg, A. G., Hughen, K. A., Kromer, B., Manning, S. W., Muscheler, R., Palmer, J. G., Pearson, C., van der Plicht, J., Reimer, R. W., Richards, D. A., Scott, E. M., Southon, J. R., Turney, C. S., Wacker, L., Adolphi, F., Büntgen, U., Capano, M., Fahrni, S. M., Fogtmann-Schulz, A., Friedrich, R., Köhler, P., Kudsk, S., Miyake, F., Olsen, J., Reinig, F., Sakamoto, M., Sookdeo, A., and Talamo, S.: The IntCal 20 Northern Hemisphere Radiocarbon Age Calibration Curve (0–55 cal kBP), Radiocarbon, 62, 725–757, https://doi.org/10.1017/RDC.2020.41, 2020.

Salvador, P.-G., Berger, J.-F., Fontugne, M., and Gauthier, E.: Etude des enregistrements sédimentaires holocènes des paléoméandres du Rhône dans le secteur des Basses Terres (Ain, Isère, France), Quaternaire, 16, 315–328, https://doi.org/10.4000/quaternaire.517, 2005.

Scapozza, C.: L'evoluzione degli ambienti fluviali del Piano di Magadino dall'anno 1000 a oggi, Arch. Stor. Ticin., 153, 60–92, 2013.

Scapozza, C.: Appunti climatici e glaciologici sulle descrizioni della Valle di Blenio tra Settecento e Ottocento, Arch. Stor. Ticin., 155, 38–63, 2014.

Scapozza, C.: Evidence of paraglacial and paraperiglacial crisis in Alpine sediment transfer since the Last Glaciation (Ticino, Switzerland), Quaternaire, 27, 139–154, https://doi.org/10.4000/quaternaire.7805, 2016.

Scapozza, C.: Esempi di corrispondenze della suddivisione formale della Serie/Epoca dell'Olocene nella Svizzera italiana, Boll. Soc. Ticin. Sci. Nat., 107, 83–88, 2019.

Scapozza, C. and Ambrosi, C.: Between glaciers, rivers and lakes: the geomorphological landscapes of Ticino, in: Landscapes and Landforms of Switzerland, edited by: Reynard, E., Springer Nature, Cham, Switzerland, 325–336, https://doi.org/10.1007/978-3-030-43203-4_22, 2021.

Scapozza, C. and Czerski, D.: Geomorfologia della Svizzera italiana/Die Geomorphologie der Südschweiz, Archeol. Schweiz, 42, 8–13, https://doi.org/10.5169/seals-860436, 2019.

Scapozza, C. and Oppizzi P.: Évolution morpho-sédimentaire et paléo-environnementale de la plaine fluvio-deltaïque du Ticino pendant l'Holocène récent (Canton du Tessin, Suisse), Géomorphologie, 19, 265–286, https://doi.org/10.4000/geomorphologie.10289, 2013.

Scapozza, C., Riff., F., and Schoeneich, P.: Stratigraphie, paléogéographie et dynamique tardiglaciaire du Quaternaire ancien de la Côte entre Gilly et Bursins (VS), Bull. Soc. Vaud. Sc. Nat., 91, 343–361, https://doi.org/10.5169/seals-282157, 2009.

Scapozza, C., Castelletti, C., and Czerski, D.: Nuove datazioni per la storia dell'evoluzione olocenica degli ambienti fluviali del Piano di Magadino (Cantone Ticino, Svizzera), Boll. Soc. Tic. Sci. Nat., 105, 97–102, 2017.

Schoeneich, P.: Le retrait glaciaire dans les vallées des Ormonts, de l'Hongrin et de l'Etivaz (Préalpes vaudoises), Travaux & Recherches, 14, Institut de Géographie de l'Université de Lausanne, Lausanne, Suisse, p. 483, 1998.

Sormani, M. A.: La necropoli leponzia di Gudo: le tombe golasecchiane (VI–V sec. a. C.), Boll. Stor. Svi. It., 110, 113–134, 2007.

Sormani, M. A.: La necropoli protostorica di Gudo: dall'epoca del Bronzo alla seconda età del Ferro, Boll. Ass. Archeol. Ticin., 24, 4–7, https://doi.org/10.5169/seals-391551, 2012.

Sormani, M. A.: La necropoli protostorica di Gudo: dall'epoca del Bronzo alla seconda età del Ferro, Rivista archeologica dell'antica provincia e diocesi di Como, 193/194, 5–160, 2013.

Strunk, A., Olsen, J., Sanei, H., Rudra, A., and Larsen, N. K.: Improving the reliability of bulk sediment radiocarbon dating, Quaternary Sci. Rev., 242, 106442, https://doi.org/10.1016/j.quascirev.2020.106442, 2020.

Tinner, W., Hubschmid, P., Wehrli, M., Ammann, B., and Conedera, M.: Long-term forest fire ecology and dynamics in southern Switzerland, J. Ecol., 87, 273–289, https://doi.org/10.1046/j.1365-2745.1999.00346.x, 1999.

Tinner, W., Lotter, A. F., Ammann, B., Conedera, M., Hubschmid, P., van Leeuwen, J. F., and Wehrli, M.: Climatic change and contemporaneous land-use phases north and south of the Alps 2300 BCE to 800 CE, Quaternary Sci. Rev., 22, 1447–1460, https://doi.org/10.1016/S0277-3791(03)00083-0, 2003.

UFAM: Rivalutare i corsi d'acqua – per l'uomo e la natura, UFAM – Ufficio federale dell'ambiente, Berna, Svizzera, p. 32, 2017.

Wirth, S. B., Glur, L., Gilli, A., and Anselmetti, F. S.: Holocene flood frequency across the Central Alps – solar forcing and evidence for variations in North Atlantic atmospheric circulation, Quaternary Sci. Rev., 80, 112–128, https://doi.org/10.1016/j.quascirev.2013.09.002, 2013.

Zumbühl, H. J. and Holzhauser, H.: Glaciers des Alpes du Petit âge glaciaire, Les Alpes, 3, 1–322, 1988.